LYNDS 379 - a new source of bipolar molecular flow

Astron. Astrophys. 154, 274–278 (1986)

ASTRONOMY AND ASTROPHYSICS

Lynds 379: a new source of bipolar molecular flow

John Hilton [1], Glenn J. White [2], Nigel J. Cronin [3], and Ruth Rainey [2]

[1] Department of Mathematical Sciences, Goldsmiths' College, University of London, New Cross, London SE14 6NW, England
[2] Astrophysics Group, Department of Physics, Queen Mary College, University of London, Mile End Road, London E1 4NS, England
[3] School of Physics, University of Bath, Claverton Down, Bath BA2 7AY, England

Received July 8, accepted July 13, 1985

Summary. A study has been made incorporating molecular line CO $J=2-1$ and optical star counting techniques of the sharp-edged Lynds dark cloud 379. It is found to lie at a distance of 200 pc, and to have an average extinction, A_B, of <2 mag. Molecular mapping has revealed the presence of a new bipolar molecular flow source coincident with a strong IRAS far infrared peak. This indicates the presence of active star formation at the edge of the cloud – possibly as a consequence of the mechanism (such as an interstellar shock) which has led to compression of the edge of L379.

Key words: planetary nebulae: L379

1. Introduction

An inspection of the National Geographic Society – Palomar Sky Atlas and the ESO/SRC Southern Sky Atlas plates reveals a number of interesting dark clouds which have very sharp edges extending over lengths of up to ~1 pc. This may represent evidence of compression of the outside of the cloud by some as yet unspecified interstellar shock wave process.

An example of such an object is L379. Figure 1 shows an enlargement made from plate J5102 of the ESO/SRC Southern Sky Survey to indicate the object and its general environment.

In order to improve our understanding of L379 we have studied it using a combination of CO $J=2-1$ molecular line observations, IRAS point source survey data, and star counting techniques.

2. Optical star counting

2.1. Star count measurements

During recent years there have been several examples of the use of star counts in the study of dark clouds (Coulson et al., 1978; Mattila, 1979; Minn and Greenberg, 1979; Saito, 1981; Sandell, 1981; Duerr and Craine, 1982; Gaida et al., 1984). In the present paper star counts are used to determine the spatial extent and extinction of L379 and an attempt is made to estimate the cloud distance. The COSMOS measuring machine at the Royal Observatory, Edinburgh was used to count stars in a raster scan mode for a $1^\circ.8 \times 1^\circ.5$ area on the UK Schmidt blue plate centred on Right Ascension (1950) $= 18^h20^m$ and Declination (1950) $= -15°$. The COSMOS machine was used in the threshold mapping mode with off-line image analysis. A total of approximately 125,000 images were counted in this area and since the field was very crowded it proved necessary to impose a 40 % threshold cut above the background. Subsequent reduction and analysis of the COSMOS data were carried out on a VAX 11/750. The analysis of the COSMOS data proceeded as follows:

2.2. Star count and extinction data

Star counting was carried out to determine the number of stellar images, N, contained in $1' \times 1'$ cells located relative to an arbitrary origin (all subsequent references to offsets will be relative to this point) at Right Ascension (1950) $= 18^h27^m00^s$ and Declination (1950) $= -15°10'00''$ as shown in Fig. 2. A contour line is drawn on Fig. 2 for $N=10$ to indicate the cloud boundary. Included on the diagram the small filled circles represent the points at which molecular line data were subsequently obtained.

Following the procedure of Dickman (1978) the raw star counts given on Fig. 2 were converted into extinctions, A_B, relative to a maximum star count of 23 observed at a position close to, but away from L379, for which the extinction due to L379 was considered to be zero. The resulting extinction map is shown in Fig. 3, drawn on the same grid as Fig. 2. A contour line is drawn along the cloud boundary for $A_B=1$. A simple comparison between the boxed area on the cloud and the boxed area off the cloud reveals an *average* extinction of approximately 1.7 mag for the cloud relative to its adjacent background.

2.3. Cumulative luminosity functions and cloud distance

In addition to star counting, cumulative luminosity functions (Wolf, 1923) were estimated for the cloud and its immediate neighbourhood, where for each grid cell on the cloud the number of stars, $N(m)$, per square cm of the plate, which had a magnitude brighter than apparent magnitude m, were estimated. In the absence of a photoelectric sequence, thirteen stars from the SAO catalogue on the same plate were used to provide a first order calibration of the corresponding COSMOS stellar images, each of area A, in terms of the SAO apparent visual magnitude m. A least-squares straight line fit showed that

$$m = -3.55 \log_{10} A + 21.8 .$$

Send offprint requests to: J. Hilton

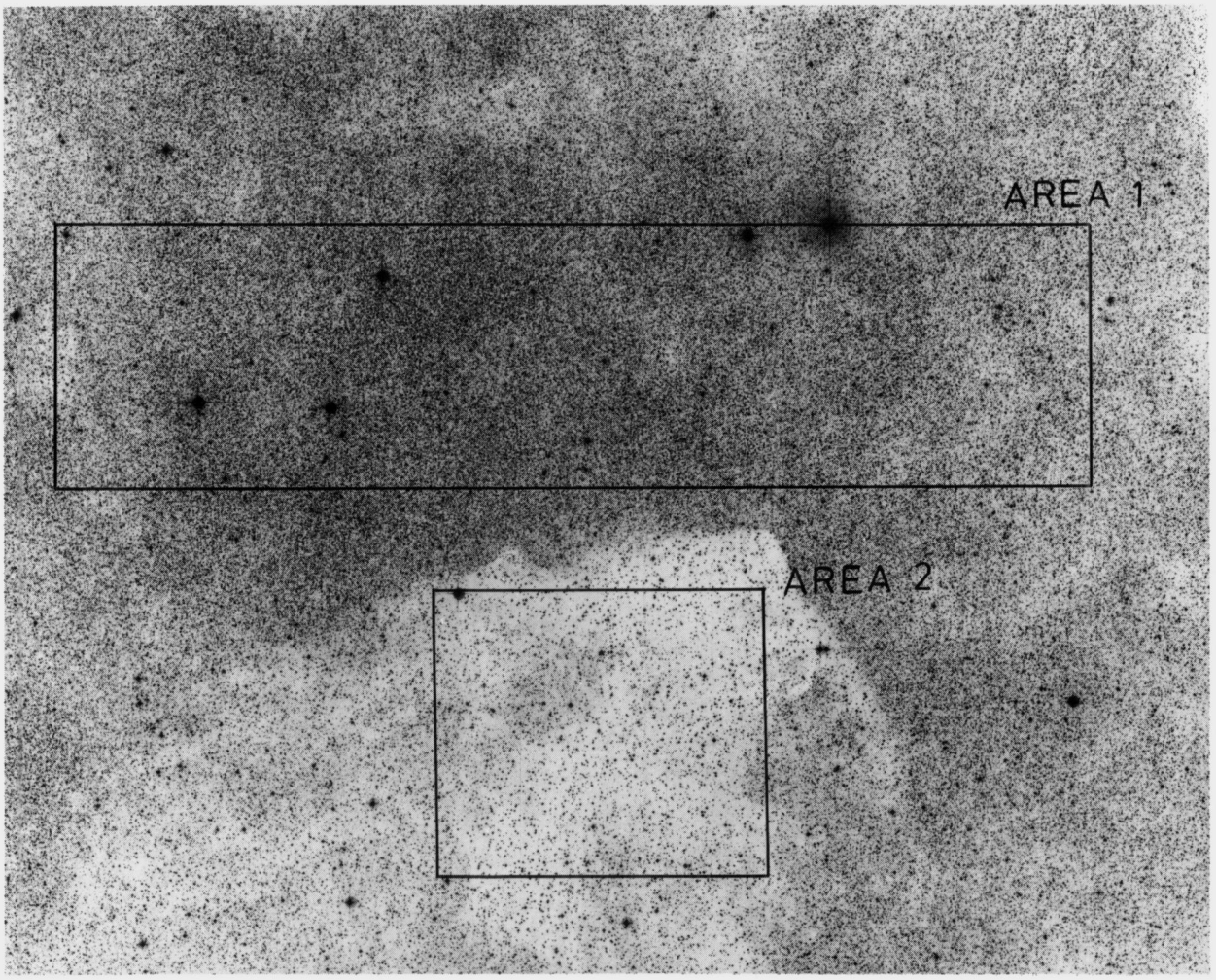

Fig. 1. L 379 shown on an enlargement from ESO/SRC Southern Sky Survey field No. 662

The SAO magnitude range used extends from 5.7 to 9.2, but considering the results of Dodd et al. (1977) it was considered reasonable to make a linear extrapolation to $m = 12.5$. Figure 4 shows the Wolf diagrams determined for areas 1 (crosses) and 2 (diamonds) of Fig. 1: 42,000 stars were counted in area 1 and 8900 were counted in area 2. The error bars drawn on the Wolf diagram are given as $n^{1/2}$ where n is the number of stars counted. To avoid confusion only one error bar is shown for the points at $m = 8.5$ and where no error bars are shown the uncertainty is considered negligible. It was found necessary to avoid the area around γ–Scu for star counting purposes as the off-line image analysis indicated a rather confused picture of intensity distribution.

Our interpretation of Fig. 4 is as follows.

1. Stars with an apparent magnitude $> m \sim 9$ are affected by absorbing material and taking the distance of a 9th magnitude star as ~ 200 pc (Allen, 1973), then the cloud must be at a distance of $\leqq 200$ pc and probably at (200 ± 50) pc.

2. For the approximately linear portion of the graph between $m = 9.0$ and 11.5 the slope of the graph is significantly greater than the slope of the graph for the corresponding data for the off-cloud position (represented by triangles on Fig. 4) according to Allen (1973). Taking the distance of a star of magnitude 11.5 as 320 pc it appears that the region between distances of approximately 200 pc and 320 pc is more populous than expected and that the star density may be higher than on average for this region of the galactic plane.

3. For stars fainter than for $m = 11.5$ the slope of the graph gradually decreases indicating a possible gradual increase in the proportion of low luminosity stars – or alternatively it could be interpreted as evidence of the difficulties which arise when an attempt is made to count faint stars in a crowded field. Such a trend has been seen in the data of Coulson et al. (1978).

3. Molecular line observations

A region of L379 was mapped in the CO $J = 2 - 1$ transition at UKIRT. The observations were obtained with the QMC Millimetre/Submillimetre heterodyne spectrometer mounted at the $f/8$ focus of the United Kingdom Infrared Telescope, Hawaii. The data consisted of 5 min integrations at 77 positions within the globule. In Fig. 5 contours of peak T_R^* are shown. A single temperature peak with $T_R^* = 13.2$ K is seen, centred at Right Ascension (1950) $= 18^h26^m35^s.5$. Declination (1950) $= -15°18'00''$. For an extended source with diameter $> 3'$, this corresponds to a kinetic temperature, T_{KIN}, of 18 K. A velocity gradient of $\sim 10\,\mathrm{km\,s^{-1}\,pc^{-1}}$ in a NW–SE direction is observed across this hot spot as determined from the velocity of peak T_R^* on the spectrum.

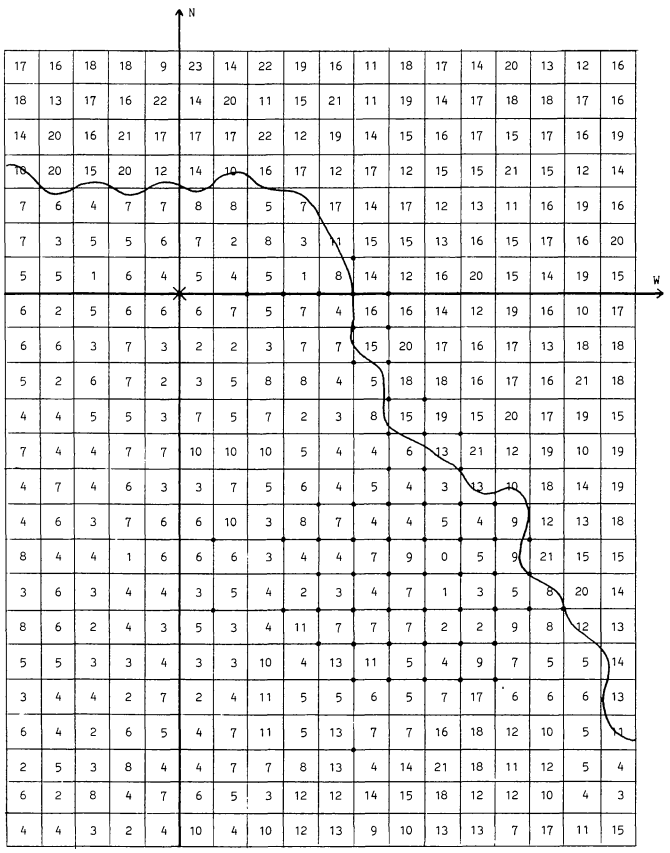

Fig. 2. Star count data for L 379 showing the number of stars counted in 1′ × 1′ squares for the region studied. The grid calibration is at intervals of 1′ relative to the origin × at Right Ascension (1950) = 18^h27^m, Declination (1950) $-15°10'$

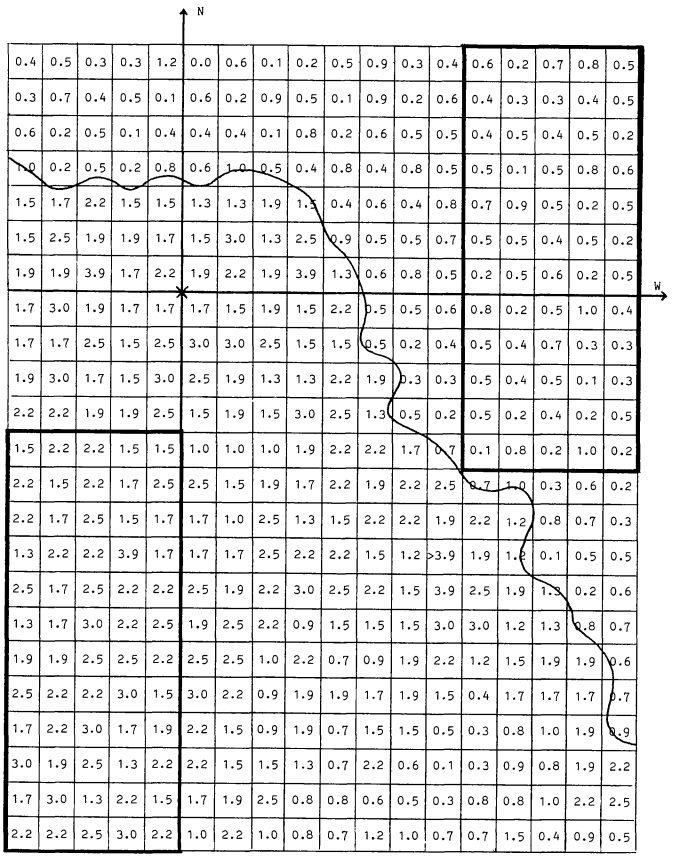

Fig. 3. Extinction data for L 379 showing the number of magnitudes of extinction relative to an extinction of zero for a star count of 23 on Fig. 2. The grid is identical with that defined in Fig. 2

The section of the L379 cloud to the north has a more constant velocity $\sim +20\,\mathrm{km\,s^{-1}}$. The temperature contours to the NW show a rapid decline of T_R^* which occurs across the edge of the sharp rim of L379 seen in the optical data. At positions away from the temperature peak, T_R^* is typically ~8–9 K, indicating T_{KIN} ~13–14 K. This is similar to that found for many other dark clouds (Young et al., 1982; Snell, 1981).

In Fig. 6 the half intensity linewidth is seen to peak close to the position of maximum T_R^* and the region of maximum linewidth ($\Delta V \sim 7\,\mathrm{km\,s^{-1}}$) runs for a total of ~(0.25 pc) in a N–S direction. When the integrated line emission in the wings of the CO line are integrated for velocities less than $14.5\,\mathrm{km\,s^{-1}}$ (the blue wing) or greater than $22.5\,\mathrm{km\,s^{-1}}$ (the red wing), the source is seen to exhibit a bipolar spatial structure, as seen in Fig. 6. The separation between the two lobes is ~2′.7, corresponding to ~0.16 pc. This bipolar structure is indicative of a molecular flow source associated with the temperature hot spot. The redshifted flow lobe is coincident with the hot spot, whereas the blushifted lobe lies some 2–3′ to the south.

Observations towards a number of other molecular flow sources associated with dark clouds have been reported by Goldsmith et al. (1984) and by Avery et al. (1985). In order to estimate the physical properties of the flow in L379, we will adopt an *average* density n_{H_2} of $2\,10^3\,\mathrm{cm^{-3}}$ as relevant to the flowing gas (based on observations reported by Avery et al. (1985) for B335 and L723). We then find that assuming each lobe is filled with flow gas, then each of the flow-lobes contains $\sim 0.9\,M_\odot$ of gas. The dynamical time scale for the lifetime of this source will be

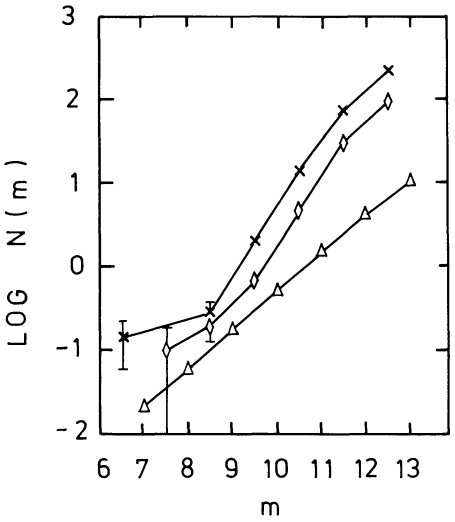

Fig. 4. Wolf diagram for region 1 (crosses) and region 2 (diamonds) of Fig. 1 where N(m) is the number of stars counted per cm^2 of plate area brighter than apparent magnitude *m*. The corresponding mean values according to Allen (1975) are indicated by triangles

$\leqq 2.4\,10^4$ yr, the force required to drive the flow is $\sim 5.6\,10^{-4}\,M_\odot\,\mathrm{yr^{-1}\,km\,s^{-1}}$, and the total mechanical luminosity in the flow is $\sim 0.35\,L_\odot$. It is notable that both the size of the L379 flow, and its physical parameters, are very similar to the L1551 flow, although in L379, the flowing material is less collimated.

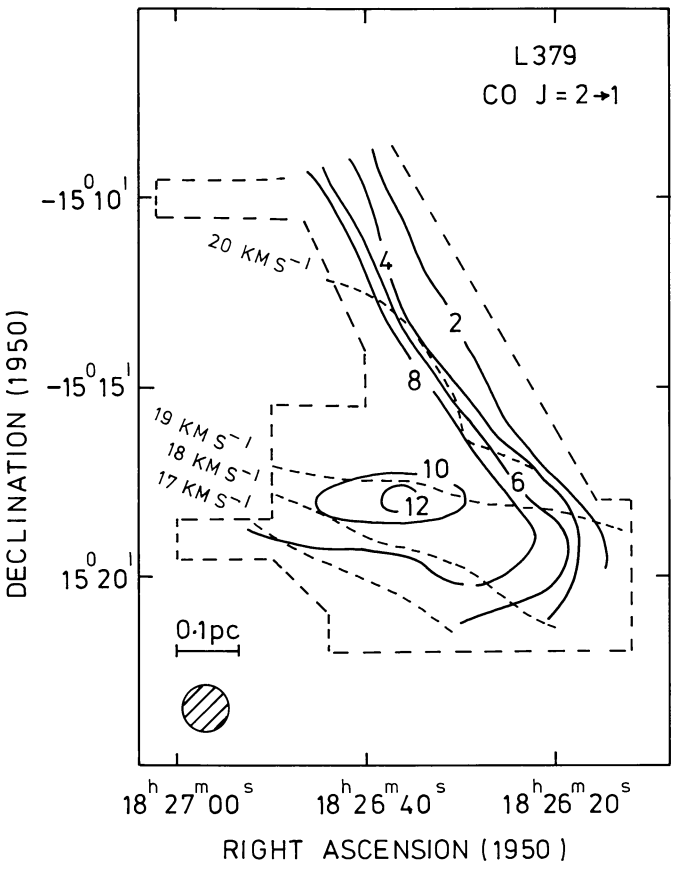

Fig. 5. Contours (solid lines) of T_R^* seen towards L 379. [For comparison T_R^* (Orion) = 82 K], superimposed with (dotted lines) the peak line velocity (km s^{-1})

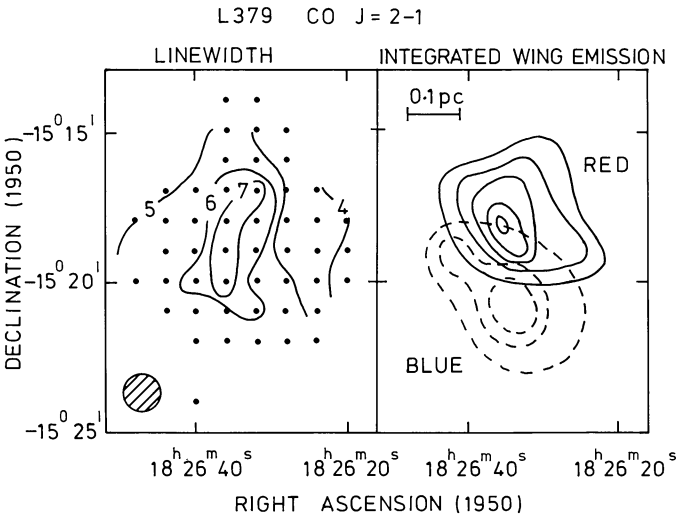

Fig. 6. Maps of the half power linewidth (km s^{-1}) and the integral of T_R^* in the line wings (in units of K km s^{-1} × 0.65) as defined in the text. The minimum contour is 1.6 K km s^{-1} and the increments are at 1.6 K km s^{-1} intervals. The bipolar nature of this section of L 379 is readily apparent

4. IRAS observations

Inspection of the IRAS point source catalogue shows 17 objects lying close to the L379 region, within a box of ±20′ in Right Ascension and ±10′ in Declination [relative to Right Ascension (1950) = 18^{h}27^{m}30^s, Declination (1950) = −15°19′00″.] Of these candidate IR sources, only three are both strong (>300 Jy) at 100 μm and show far IR spectra which rise very sharply at the longer wavelengths. In Table 1 we list these objects and their IRAS fluxes.

The objects labelled (1) and (2) lie close together separated from each other by ~40″. Between these two objects a small patch of nebulosity can be seen on the POSS print. The shape of the IR spectrum coupled with the presence of the patch of nebulosity would suggest these IR sources to be associated with an embedded cool object of blackbody temperature $\lesssim$40 K.

The IRAS source 3, the strongest 100 μm object in the whole area, is coincident with the CO hot spot we have discovered, and lies at the centre of the red flow lobe. It would seem likely that this infrared object may indicate the position of the source responsible for driving the molecular flow. We have attempted to fit the observed IRAS fluxes for L379 (3) with single temperature models of dust emission with the dust emissivity $\alpha\nu$. No acceptable fits were found. Inspection of the IRAS fluxes indicated the presence of dust at $T \sim 65$ K (from the ratio of 12 to 25 μ fluxes) and $T < 30$ K (from the ratio of 60 to 100 μ fluxes). Although estimates of the luminosities of objects as cool as this may be somewhat uncertain due to the colour corrections which need to be made to the IRAS data, we can estimate a *lower* luminosity for the IRAS source of 40 $L_\odot$. This luminosity would correspond to a ZAMS star of class ~B9. If the object were a main sequence star, then we would expect the apparent visual magnitude to be $\sim +7$. No object is visible on either the red or the blue POSS prints at the position of the IRAS source, implying either that $A_v \gtrsim 15$ mag, or that the star is in a protostellar phase of evolution. However it is unlikely that a mainsequence star would have remained embedded in its parent globule for so long without escaping its parent cloud.

5. Discussion

One of the interesting aspects of this embedded flow is the close proximity to the sharp edge of the dark cloud. As seen in Fig. 1, the rim extends ~2.5 pc SW–NE, and $\gtrsim$1 pc E–W. We speculate that the presence of these sharp edges may be indicative of shock-wave compression of the edge of the dark cloud. The POSS plates have

Table 1

	RA	Dec	Flux (Jy)			
			12 μ	25 μ	60 μ	100 μ
L379 (1)	18 27 42.1	−15 17 17	3.58	4.12	<147.2	350.6
(2)	18 27 43.4	−15 16 45	<3.58	<2.14	147.24	389.64
(3)	18 26 32.9	−15 17 51	<1.5	46.4	445.1	1297.1

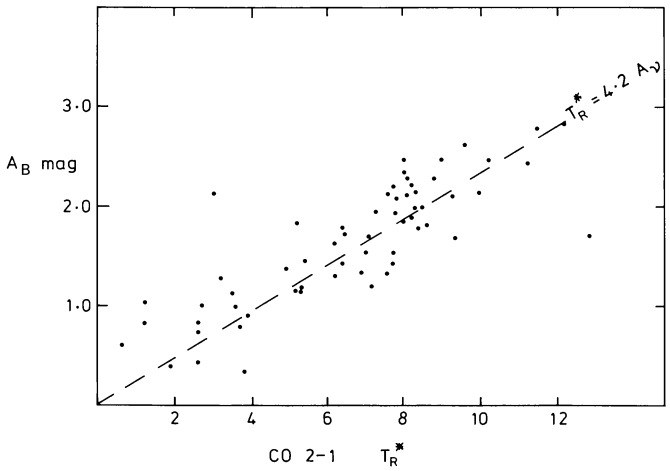

Fig. 7. Variation of T_R^*(K) width with A_B (magnitudes). A best-fit with $T_R^* = \sim 4.2 A_B$ is found

been searched to look for any possible shock wave progenitors which could compress the cloud edge, such as nearby intense young stars of H II regions, but nothing obvious can be seen. The Serpens OB1/OB2 association lies some four degrees to the NW of L379. Based on the kinematic distance determined from CO measurements of ~2 kpc (Blitz et al., 1982), an association with L379 is unlikely which could have resulted in a dynamical interaction. IC 4703 lies ~3° NW of the western side of L379, but no distance measurements are available.

Observations of shock compressed bright rims of a number of clouds have been reported by Wootten et al. (1983). The major difference between Wootten's objects and L379 is that no obvious bright star lies nearby, and no bright rim is seen. There is no evidence in the L379 data for an enhancement of the red wing across the rim as reported for NGC 1977 and IC 1396 by Wootten et al. (1983). Hydromagnetic calculations by Sanford et al. (1984) indicate that there are no objections to structures resembling L379, although we can see no obvious progenitor source which could lead to compression of the edges of the globules. In addition. no evidence for changes to the linewidth or shape of the spectrum are seen at the edges of L379, whereas we note for other objects (M17, Rainey et al., 1986; W80, Bally and Scoville, 1980) that such changes are often seen as a result of shock wave interaction with neutral material.

In order to examine the variation of CO temperature with position in the cloud, we have plotted in Fig. 7 the variation of T_R^* $(J=2-1)$ with A_B, where A_B has been averaged over 1 square arc minute areas appropriate to the position of the individual CO spectra. A clear trend of T_R^* *and* A_B is seen with T_R^* (CO $J=2-1$) $= \sim 4.2\, A_B$ for A_B up to ~3 mag. No evidence for heating of the CO as a result of ultra violet heating of the cloud edges by background starlight for low A_B is seen, although it is likely that variation of T_R^* will be a complex function of density, abundance and excitation gradients at the cloud edge.

6. Conclusions

1. Using star counting techniques the distance to the sharp edged dark cloud L379 is found to be (200 ± 50) pc.

2. A new bipolar molecular flow source has been discovered lying just inside one of the sharp rims. This object is similar in characteristics to other low luminosity molecular flows seen in dark clouds.

3. Several intense IRAS 100 μm sources are found inside L379; one of these is associated with the molecular flow source and has a luminosity $> 40\, L_\odot$.

4. It is likely that the sharp edges to the L379 have resulted from an external shock wave compression. If the shock velocity is $\gg$ the sound speed in the neutral gas, it is possible that the shock lies inside the dark cloud to the east of the observed optical rim, and may have been associated with the star formation revealed by the detection of the bipolar molecular flow. The source of this possible shock is as yet unknown.

Acknowledgements. We gratefully acknowledge: the COSMOS unit at the Royal Observatory, Edinburgh for the help in obtaining the star count data; the staff of UKIRT for operations of UKIRT and telescope assisting; the SERC for financial support for observing, and also for the support of Millimetre/Submillimetre astronomy and receiver development at QMC: PATT for allocation of observing time.

References

Allen, C.W.: 1974, Astrophysical Quantities, The Athlone Press, London
Avery, L.W., White, G.J., Williams, I.P., Cronin, N.J.: 1985, *Astrophys. J.* (in press)
Bally, J., Scoville, N.Z.: 1980, *Astrophys. J.* **239**, 121
Blitz, L., Fich, M., Stark, A.A.: 1982, *Astrophys. J. Suppl.* **49**, 183
Coulson, I.M., Murdin, P.G., MacGillivray, H.T., Zealey, W.J.: 1978, *Monthly Notices Roy. Astron. Soc.* **184**, 171
Dickman, R.L.: 1978, *Astron. J.* **83**, 363
Dodd, R.J., MacGillivray, H.T., Hilditch, R.W.: 1977, *Monthly Notices Roy. Astron. Soc.* **181**, 729
Duerr, R., Craine, E.R.: 1982, *Astron. J.* **87**, 408
Gaida, M., Ungerechts, H., Winnewisser, G.: 1984, *Astron. Astrophys.* **137**, 17
Goldsmith, P.F., Snell, R.L., Hemeon-Heyer, M., Langer, W.D.: 1984, *Astrophys. J.* **286**, 599
Mattila, K.: 1979, *Astron. Astrophys.* **78**, 253
Minn, Y.K., Greenberg, J.M.: 1979, *Astron. Astrophys.* **77**, 37
Rainey, R., White, G.J., Gatley, I., Hayashi, S., Kaifu, N.: 1986, *Astron. Astrophys.* (submitted)
Saito, T., Ohtani, H., Tomita, Y.: 1981, *Publ. Astron. Soc. Japan* **33**, 327
Sandell, G., Johansson, L.E.B., Nguyen-Q-Rieu, Mattila, K.: 1981, *Astron. Astrophys.* **97**, 317
Sanford, M.T., Whitaker, R.W., Klein, R.I.: 1985, *Astrophys. J.* **282**, 178
Snell, R.L.: 1981, *Astrophys. J. Suppl.* **45**, 121
Wolf, M.: 1923, *Astron. Nach.* **219**, 109
Wootten, A., Sargent, A., Knapp, G.R., Huggins, P.J.: 1983, *Astrophys. J.* **269**, 147
Young, J.S., Goldsmith, P.F., Langer, W.D., Wilson, R.W., Carlson, E.R.: 1982, *Astrophys. J.* **261**, 513

Note added in proof: Recent (August 1985) CO $J=2-1$ observations (White et al. in preparation) have mapped a small area around the positions of the other IRAS sources indicated in Table 1. The CO $j=2-1$ lines typically have $T_R^* \sim 10$–12 K at $V_{lsr} = 20.2\ \mathrm{km\,s^{-1}}$ and a half power linewidth of $\sim 3\ \mathrm{km\,s^{-1}}$. There is some evidence for position dependent asymmetry in the line shapes, suggesting some dynamic interaction between the infrared sources and the surrounding gas.